UDC 669.017:539.16

COOPERATIVE EFFECT OF DISPLACEMENT DAMAGE AND INERT GAS IMPURITIES ON DEUTERIUM RETENTION IN AUSTENITIC AND FERRITIC-MARTENSITIC STEELS

S.A. Karpov, I.E. Kopanets, V.V. Ruzhytskyi, B.S. Sungurov, G.D. Tolstolutskaya
National Science Center "Kharkov Institute of Physics and Technology", Kharkov, Ukraine

The behaviour of hydrogen (deuterium) in austenitic 18Cr10NiTi stainless steel and ferritic/martensitic steels EP-450 and EI-852 were investigated. Energetic heavy-ion irradiation has been used for modeling defect cluster formation under displacement cascade conditions to simulate nuclear-power environments. The influence of preimplanted argon on deuterium trapping in steels was studied using methods of ion implantation, the nuclear reactions $D(^3He,p)^4He$, thermal desorption spectrometry and transmission electron microcopy. It was found that retention of deuterium in steels is strongly enhanced by presence of radiation damages created by argon ions irradiation. The hydrogen release temperature interval shifts on 200 K to higher temperature. For the obtaining of deuterium trapping and desorption thermodynamic parameters in steels numerical simulation on the base of the continuum rate-theory was used.

INTRODUCTION

Hydrogen plays a significant role in the evolution of damage microstructure and may affect the mechanical properties and cracking behavior of structural materials. The conclusions for nuclear power reactors, especially in the environments where the irradiation induced defects are introduced and simultaneously hydrogen is introduced due to the existence of nuclear transmutation in the steel, are as follows: the implanted hydrogen ions had a significant effect on the microstructural damage at the initial stage of irradiation [1]. Hydrogen enhanced the nucleation but inhibited the growth of the dislocation loops. Hydrogen could greatly improve the effective nucleation sites of voids, but inhibit their growth. The formation of voids with small size and high number density should be concerned closely with fast diffusion rate, low migration activation energy and trapping of vacancies by hydrogen atoms during irradiation.

In addition to plasma contamination concerns, hydrogen retention is also a critical issue for ITER, as it can affect fuelling efficiency, plasma density control, and tritium inventory and permeation through the wall or into coolant channels. Therefore, the underlying mechanism of hydrogen trapping in structural materials has been widely studied, but with inconsistent results, especially when it comes by means of ion fluence and specimen is exposed to the complex temperature dependence.

Results obtained in paper [2] for 18Cr10NiTi stainless steel show that ion implanted deuterium is weakly trapped by defects produced in 5 keV D^+ displacement cascades. The effective trapping temperature interval is 300…600 K. Helium implantation into this steel causes the formation of traps that can retain hydrogen isotopes in a wider range of temperatures, 500…1000 K. The characteristics of trapping and the temperature range of retention of hydrogen isotopes in traps formed by prior implantation of helium depend on the implanted helium concentration and on the developed defects type. Helium bubbles formation in 18Cr10NiTi steel causes an increase of retained deuterium by one order of magnitude in the range 350…550 K.

Results obtained for stainless steel 18Cr10NiTi shown that pre-irradiation of argon and the damage creation at the level of 100…200 dpa provides the accumulation and retention of approximately all deuterium implanted at room temperature to concentrations of 3000 to 15000 appm [3]. Summarizing the results it can be stated that helium and argon implantation into austenitic stainless steel 18Cr10NiTi caused the formation of traps that retain hydrogen isotopes to temperatures of about 1000 K. The interaction between deuterium and argon ion-induced displacement damages is not strong compared with inert gas bubbles.

In the current study we investigate hydrogen retention and release from austenitic and ferritic-martensitic steels, the influence of radiation damage on accumulation and distribution of deuterium implanted in steels after annealing and implantation at high temperature.

1. EXPERIMENTAL PROCEDURE

The specimens used were foils of austenitic 18Cr10NiTi and ferritic-martensitic steels EP-450 (Cr13Mo2NbVB), EI-852 (Cr13Mo2VS). Specimen dimensions were 27×7×0.1 mm. These specimens were polished in electrolyte having composition: 54% H_3PO_4, 11% H_2SO_4, 21% H_2O, and 14% CrO_3 or $HClO_4$ (10%) + $C_3H_8O_3$ (10%) + C_2H_5OH (80%). Before irradiation the specimens were short-term annealed in the experimental chamber for surface cleaning and degassing. Composition of investigated materials is presented in the Table. The initial structure of steels EP-450, EI-852 and 18Cr10NiTi is shown on Fig. 1. Microstructure of steel EP-450 consisted of a duplex the structure of tempered martensite (sorbite) and ferrite of approximately 1:1. Along the grain boundaries ferrite-ferrite and ferrite-sorbite observed large globular carbides $M_{23}C_6$ with a strong contrast in bright-field image and smaller carbides on the boundaries of martensite grains. Globular carbides $M_{23}C_6$ observed in initial structure of steels EI-852.

Grade of steel	Country producer	C	Si	Mn	Cr	Ni	Mo	V	W	Nb	B	Other elements
EP-450	Russia	0.1… 0.15	0.6	0.6	11… 13.5	0.05 …0.3	1.2… 1.4	0.1… 0.3	–	0.3… 0.6	0.004	–
EI-852	Russia	0.13	1.19	0.31	13.15	0.27	1.69	–	–	–	–	P = 0.017
18Cr10NiTi		≤ 0.12	0.7	1.5	18.5	10	–	–	–	–	–	0.6Ti

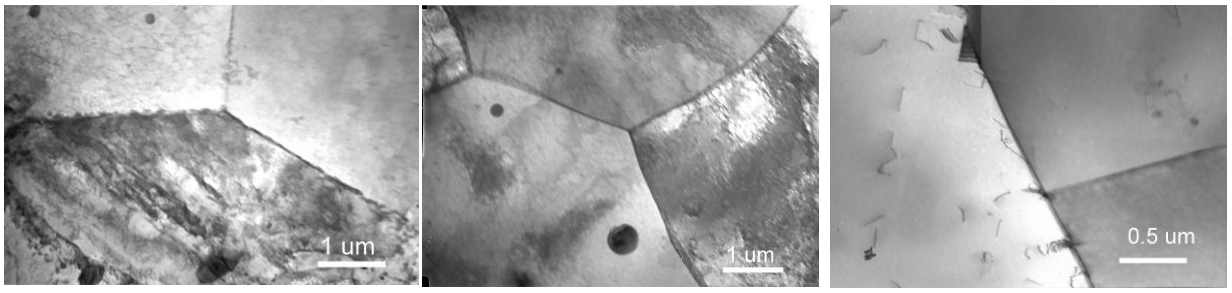

a *b* *c*

Fig. 1. Initial structure of steels EP-450 (a) and EI-852 (b) after thermal treatment 1350 K, 0,5 hour+1020 K/1 hour and microstructure of 18Cr10NiTi steel after annealing for 1 hour at 1340 K (c)

Microstructure of 18Cr10NiTi steel is two-phase after solution annealing. Grains of δ-ferrite are also observed with austenitic grains (dimension about 30 mkm). Volume fraction of δ-ferrite constitutes 2…3%. Twins of annealing precipitates of second phase (carbides and titanium carbonitrides) and dislocations are the elements of austenitic grain structure. Majority of perfect dislocation are extended on partial dislocation with stacking fault formation. Sum density of dislocation is ~ 10^8 cm^{-2}.

Combinations of nuclear reactions techniques (NRA), transmission electron microscopy (TEM), programmed thermal desorption technique (TDS) were applied to the materials in order to get a more complete picture including composition, morphology and the features of irradiation-induced defect distribution.

The measuring system "ESU-2" was used for the creation of radiation damage and measurements using different ion beam analysis techniques, including Rutherford backscattering spectroscopy (RBS), channeling, nuclear reaction analysis (NRA). The ion beam technique and methodologies for the analysis of experimental data provide a comprehensive tool for studying crystal defects.

The argon ions were chosen because irradiation with these ions with energies 0.5…1.4 MeV can cause damage production at the level of 100 to 200 dpa at a depth of 700 nm from the surface. The time to achieve 100…200 dpa was ~ 2…4 hour at the area of irradiation ~ 0.1 cm^2. Simultaneous implantation of helium and hydrogen with energies 2…50 keV may be performed by means of two irradiation facilities [3].

The assembly has an oil-free pumping system with a residual target-chamber pressure of ~ $3 \cdot 10^{-5}$ Pa. The deuterium ion flux was 10^{14} $cm^{-2} \cdot s^{-1}$. The implantation temperature ranged from 300 to 900 K. Post-implantation annealing of specimens was performed in the temperature range 300…1200 K by ohmic heating at the rate of 7 $K \cdot s^{-1}$.

The substitution of deuterium for protium allows the use of nuclear reaction profiling to determine the depth distribution and the concentration of hydrogen isotopes. Irradiations and measurements by nuclear methods were performed in one chamber, excluding contact of the specimens with air that prevented the formation of artifact trap sites associated with the surface oxide. The measurements were performed using forward and back scattering geometries.

Study of deuterium release from stainless steel was performed using a thermal desorption technique on the assembly designated "Ant" [3] in temperature range 300…1500 K at a rate of 6 $K \cdot s^{-1}$. Isotope of hydrogen deuterium was used in TDS experiments to avoid the errors caused by the influence of hydrogen evolved from components of testing chamber. The residual gas pressure in the experimental chamber was ~ $5 \cdot 10^{-5}$ Pa.

The microstructure of the implanted steels was observed using transmission electron microscopy at room temperature, employing standard bright–field techniques on an EM-125 electron microscope.

2. RESULTS AND DISCUSSION

2.1. DEUTERIUM

Fig. 2 shows deuterium distribution profiles in 18Cr10NiTi steel irradiated with 5 keV D^+ to $1 \cdot 10^{16}$ cm^{-2} at room temperature and after annealing. The amount of deuterium retained in the specimens at T_{room} was ~ 80% relative to the irradiation dose and decreases to ~ 5% after annealing up to 500 K.

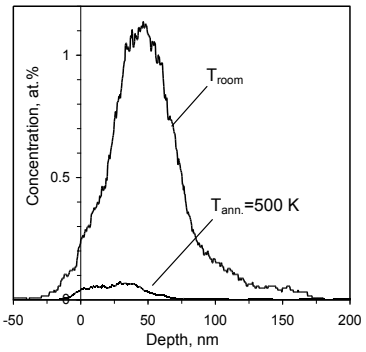

Fig. 2. Experimentally measured depth distribution profiles of deuterium implanted with energy 5 keV at T_{room} to $1 \cdot 10^{16} cm^{-2}$ in steel 18Cr10NiTi and after annealing

The nuclear reaction profiling and the thermal desorption measurements have shown that the effective temperature interval of trapping deuterium implanted in SS 18Cr10NiTi to $1 \cdot 10^{16}$ D/cm^2 is 300…600 K (Fig. 3). The data presented in Fig. 3 were obtained by using the NRA and TDS experimental techniques. A desorption is characterized by two stages of gas release with maximum at ~ 380 and 430 K.

Insert in Fig. 3 shows the exposure time dependence of deuterium retention in steel at RT after irradiation to $1 \cdot 10^{16}$ D/cm^2. It is evident, that decrease of deuterium retention is observed for the entire time interval especially drastically during the first few hours.

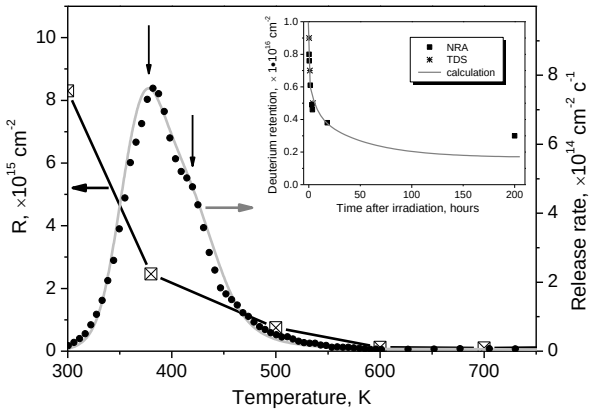

Fig. 3. Experimental (black point) and the calculated (grey curve) linear temperature ramp thermal desorptions, temperature-dependent areal densities (R) (black curve) and deuterium retention as a function of time (in insert) for 18Cr10NiTi stainless steel samples

In order to deduce the deuterium trapping parameters we have modeled the implantation, diffusion, trapping, detrapping, and recombination processes that occur during the experiment. In the model, deuterium is implanted in the sample at a distance *(x)* from the surface having the profile *G(x)* obtained from nuclear reaction profiling measurements for 5 keV D^+. The modeling calculation is a numerical solution for the diffusion of deuterium in the presence of trapping sites and has been discussed in detail elsewhere [4]. By comparison of experimental curves with calculation data it has been established that ion-implanted deuterium is trapped by radiation defects with binding energies of 0.28 and 0.36 eV. It was suggested that D atoms were trapped in vacancies and at higher doses – in vacancy clusters [4].

The calculations of deuterium retention during isothermal annealing of specimens at T = 300 K were performed with thermodynamic parameters obtained by fitting the experimental thermal desorption curve shown in Fig. 3. The modeling calculation gives a good description of the data for the exposure time of ~ 25 hours. The differences observed between the experimental and the calculated deuterium retention curves at large exposure times are related to the blocking influence of the growing superficial oxide layer. The data presented in Figs. 2 and 3 show that the ion-implanted deuterium is weakly trapped by defects produced in low-energy displacement cascades.

Depth profiles of deuterium in steel EP-450 irradiated with 5 keV D^+ to $1 \cdot 10^{16}$cm^{-2} at room temperature and its evolution during post-implantation annealing is presented on Fig. 4. Concentration of deuterium, retained in steel EP-450 at T_{room} in the implanted layer is approximately three times lower than the calculated assuming 100% trapping. The height of concentration profiles decrease during the annealing.

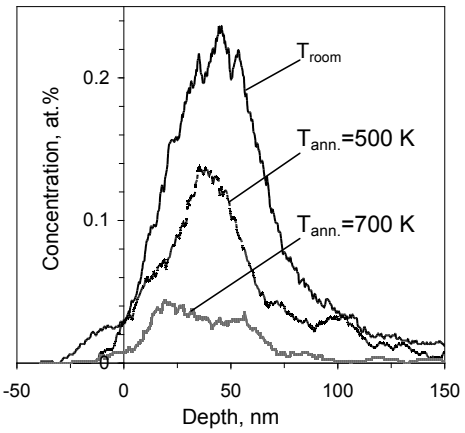

Fig. 4. Depth profiles of deuterium implanted with energy 5 keV at T_{room} to $1 \cdot 10^{16}$cm^{-2} into the steel EP-450 and after annealing

The amount of deuterium retained in the specimens and the thermal desorption measurements have shown that the higher changes are observed under the annealing in the temperature range ~ 400…500 K (Fig. 5). The temperature interval for trapping deuterium implanted in steel EP-450 to $1 \cdot 10^{16}$ D/cm^{-2} is 300…700 K and is broader than in steel 18Cr10NiTi (see Fig. 3).

In this thermal desorption measurements H_2 is used. It is known that the mass difference of deuterium and hydrogen can influence the determination of the thermal-dynamic parameters (isotope effect). However, no differences were observed in thermal desorption spectra upon change of deuterium to hydrogen.

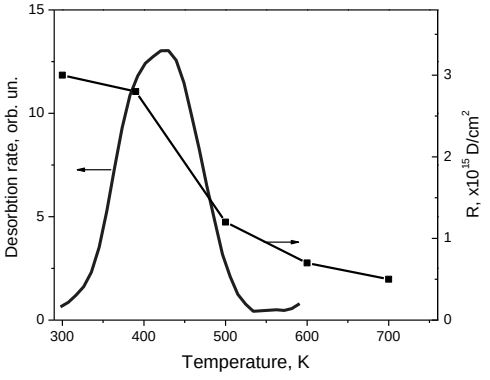

Fig. 5. Linear temperature ramp thermal desorptions for hydrogen and temperature-dependent areal densities (R) of deuterium implanted in EP-450 steel

2.2. DAMAGE + DEUTERIUM

In the present work the concentration depth profiles of retained D atoms implanted into steel were investigated as functions of the concentration of inert gas atoms and lattice disorder resulting from argon pre-

irradiation. By varying the high-energy argon implantation angle relative to the specimen we obtained different levels of damage and concentrations of argon atoms at depths between 0…1.0 μm. Marochov and Goodhew [5] have established that neon and argon can be used as an analogue for helium in implantation-and-annealing experiments, provided that the doses are adjusted so that the gas concentrations are equivalent. On the other hand, argon has a greater atomic mass than helium and it results in greater energy transfer during collisions, and thus, a higher dpa rate of target atoms.

Fig. 6 shows the influence of the 1.4 MeV Ar^+ pre-irradiation on retention of deuterium implanted in 18Cr10NiTi steel. In the backscattering geometry we increased the probing depth to 1.8 μm. The deuterium depth profiles deconvoluted from proton-energy spectra are presented. In these figure the range of argon ions calculated by the SRIM [6] code are also plotted. Distribution profile of deuterium implanted in 18Cr10NiTi steel without pre-irradiated 1.4 MeV argon ions is presented in the insert on the figure.

Preliminary creation of damages causes the retention of nearly 100% of implanted deuterium. A part of deuterium in the process of irradiation migrates in the layer of argon deposition. The process of migration affects the availability of large damages in the layer in which the deuterium is implanted.

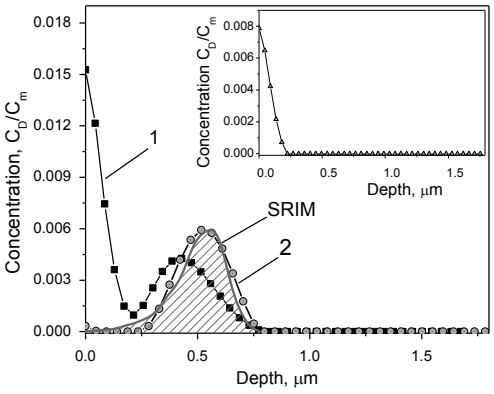

Fig. 6. Distribution profiles of deuterium implanted with energy 5 keV at T_{room} to $2.5\cdot10^{16}$ cm^{-2} in 18Cr10NiTi steel pre-irradiated with 1.4 MeV argon ions to $1\cdot10^{17}Ar/cm^2$ (1) and after annealing at 500 K (2)

After annealing at 500 K ~ 40% of the deuterium trapped in a layer of atomic displacement damage is lost, and the rest of deuterium atoms get redistributed to a greater depth completely and localized around the argon projected range. From this region the deuterium atoms escape when 18Cr10NiTi steel annealed at ~ 700 K.

Fig. 7 shows that preliminary irradiation of EI-852 steel by argon ions with energy 1.4 MeV also causes the increase of retention and redistribution of deuterium in the area of argon deposition as in the case of austenitic steel 18Cr10NiTi. Retaintion of deuterium in this case is nearly 100% at a dose of implantation $1\cdot10^{17}$ cm^{-2}.

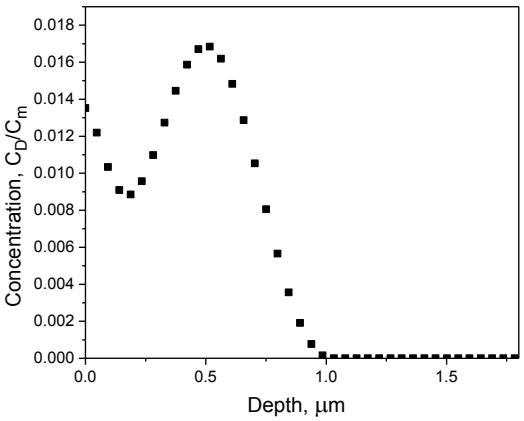

Fig. 7. Distribution profiles of deuterium implanted with energy 5 keV at T_{room} to $1\cdot10^{17}$ cm^{-2} in EI-852 steel pre-irradiated with 1.4 MeV argon ions to $1\cdot10^{17}Ar/cm^2$

Depth distribution of deuterium implanted with energy 5 keV to dose $1\cdot10^{16}cm^{-2}$ at T_{room} in EP-450 steel preliminary irradiated with 500 keV argon ions to dose $5\cdot10^{16}cm^{-2}$ and its evolution during post implantation annealing are presented on Fig. 8.

Under irradiation by argon ions with 500 keV energy the radiation damages near 100 dpa is produced with simultaneous introduction of ~ 5 at.% of inert gas on the depth of deuterium implantation (1…100 nm). It causes the retention of nearly 100% of implanted deuterium (see Fig. 8, curve 1).

Amount of deuterium and its depth distribution don't change after annealing up to 500 K. Detrapping occurs between 500 K $\leq T_{ann} \leq$ 600 K.

By processing the depth distribution profiles the values of deuterium retention in 18Cr10NiTi and EP-450 steels for all Ar-ion predimplantations were obtained. The temperature dependences of deuterium retention are shown in Fig. 9. The data of deuterium retention in specimens pre-implanted with helium are also included [2]. The calculated ion range and defect production profiles for different experimental sets are presented in the inserts

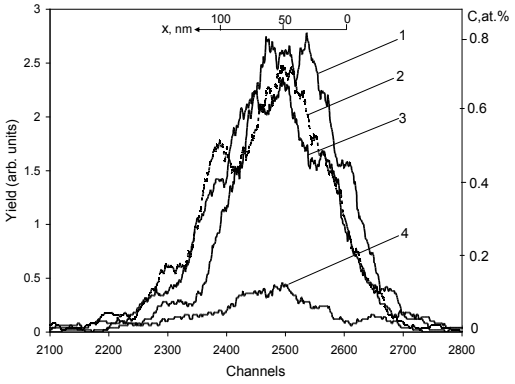

Fig. 8. Distribution profiles of deuterium implanted with energy 5 keV at T_{room} to the dose $1\cdot10^{16}cm^{-2}$ in steel EP-450 (1) after pre-irradiation 500 keV argon ions to dose $5\cdot10^{16}cm^{-2}$ and after annealing at 380 (2), 500 (3) and 600 K (4)

.

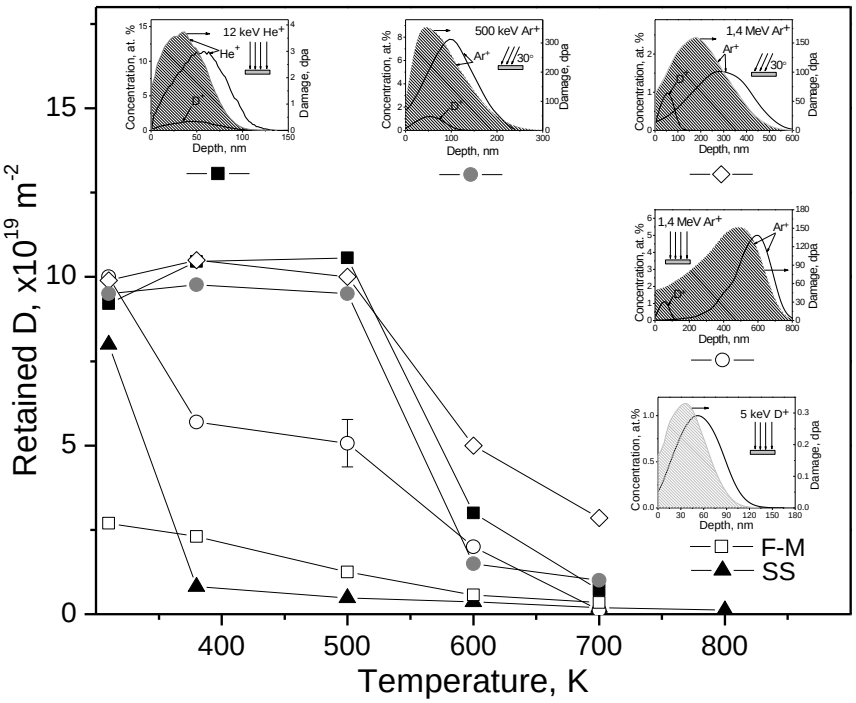

Fig. 9. Deuterium retention vs temperature in steels 18Cr10NiTi (○, ■, ◊, ▲) and EP-450 (□, ●) after irradiation by deuterium ions up to $1 \cdot 10^{16}$ cm^{-2} only (▲, □) and after argon or helium pre-implantation (○,■, ◊, ●)

As follows from a Fig. 9, depending on experimental conditions three qualitatively different types of retention behavior are observed. The behavior in one's turn is determined by efficiency of trapping strength of defects. Radiation defects produced by low energy deuterium ions are weakest traps for gas atoms and annealing of material to 500 K quite enough for most of it desorption from steels. More powerful lattice damage caused by 1.4 MeV Ar^+ ions incident perpendicular to the sample surface leads to the formation of stronger deuterium traps, so at least half of it remains in the sample after annealing to 500 K. And finally, implantation of deuterium into the layers with high level of damage and/or inert gas concentration (top three inserts on Fig. 9) causes virtually 100% deuterium retention in austenitic and ferritic-martensitic steels to annealing temperatures of ~ 500 K.

This result obtained for ions with various damaging ability (E_{He} = 12 keV, E_{Ar} = 500 and 1400 keV) imply that the actual radiation damage of the crystal lattice do not play a major role in deuterium retaining. It can be concluded that the appearance of new stronger deuterium traps in steels is due to the presence of inert gas atoms forming helium (argon) – vacancy complexes or bubbles. It is possible also that hydrogen get trapped by strained nearest bubble surrounding. The stages of sharp lowering of deuterium retention curves that are observed at temperatures $T \geq 500$ K can be connected with an essential role of surface-controlled processes with thermodynamic parameters inherent for each of steels as we think.

Published data analysis showed that in the temperature range 500…700 K structural steels are characterized by a significant increase of vacancies mobility.

In ref. [7] positron annihilation spectroscopy was used to study of the formation and annealing of vacancy clusters in austenitic steels and Fe-36%Ni alloy. Defects were induced by electron (5 MeV) irradiation at room temperature and subsequent stepwise annealing. It was shown that small vacancy clusters are formed in these materials. Vacancy clusters were thermally stable up to 450 K. For the samples preliminarily quenched for solid solution it was found that stage which associated with dissociation of vacancy-type clusters is observed between 500…650 K.

The defect recovery in proton irradiated Ti-modified D9 steel has been studied by positron annihilation isochronal and isothermal annealing measurements [8]. D9 samples have been irradiated with 3 MeV protons followed by annealing at various temperatures in range of 323 to 1273 K. The drastic decrease in positron annihilation parameters, viz. positron lifetime and Doppler S-parameter, around 500 K indicates the recovery of vacancy-type defects.

On the other hand, it is well known that irradiation of metals and alloys with inert gas ions generally results in the formation of microscopic gas bubbles even at RT [9]. For example, the microstructure is dominated by a high density of small cavities resulting from the precipitation of implanted helium for $0.6 \leq C_{He} \leq 3$ at.% [10]. Bubble growth and coalescence were observed when the temperature reached 573 K [10].

We may to suppose that similarly as it takes place at high-temperature implantation [9], during annealing of implanted specimens the processes of growth and coalescence of noble-gas bubbles occur, too. And the detrapping of hydrogen in the temperature interval 500…600 K is may be connected with bubble system transformation.

Our TEM investigations of argon-implanted 18Cr10NiTi specimen are presented in Fig. 10. A beam of 1.4 MeV argon ions was incident at angles of 30° with regard to the surface.

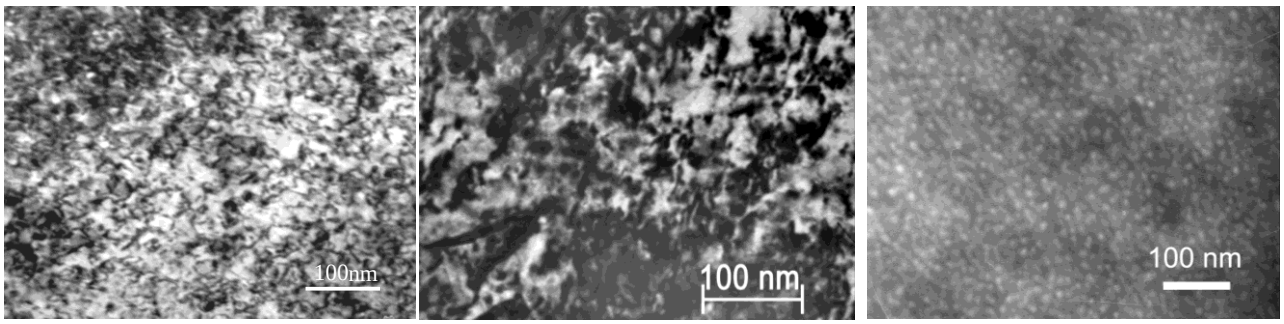

a *b* *c*

Fig. 10. Microstructure of steel 18Cr10NiTi irradiated with argon ions of 1.4 MeV energy (incident at angles of 30° with regard to the surface) to a dose of $1 \cdot 10^{17}$ cm^{-2} at room temperature (a), 600 (b) and 800 K (c)

The microstructure after irradiation at room temperature was consisted of a high density of dislocation loops and dislocation network (see Fig. 10,a). Increasing the temperature of irradiation to 600 K was caused a decreasing density of dislocation structure and a very hard-to-see bubbles (see Fig. 10,b). At $T_{irr} = 800$ K the formation of noble-gas bubbles (mean size 4 nm, density $5.5 \cdot 10^{19}$ $см^{-3}$) was observed in the implantation layer (see Fig. 10,c).

These data is allowed us to conclude that the decreasing of deuterium concentration in the temperature interval of 500...700 K probably connected with bubble system transformation caused by high mobility of vacancies at these temperatures.

CONCLUSIONS

The influence of pre-implanted inert-gas atoms on deuterium trapping in 18Cr10NiTi, EP-450 and EI-852 steels was investigated using the nuclear reactions $D(^3He,p)^4He$, desorption spectrometry and transmission electron microcopy. Trapping, retention and evolution of deuterium depth distribution profiles were studied for 10…30 keV D_2^+, 12 keV He^+ and 1.4 MeV Ar^+ implantation at room temperature followed by annealing at 300 to 1500 K. The amount of trapped and released deuterium atoms were measured as a function of implantation dose and temperature.

Retention of deuterium implanted to concentration of about 1 at.% is determined by small concentration of radiation defects created by low-energy deuterium ions, the small deuterium binding energy to defects and high hydrogen diffusivity in austenitic and ferritic-martensitic steels at room temperature. Annealing of steels up to 500 K is enough to release most of the implanted deuterium from traps.

Preliminary irradiation of steels by helium or argon ions produces strong traps including radiation damage and rare-gas atoms. As a result, the deuterium atoms retain in steel at higher temperature. The decreasing of deuterium concentration at 500…700 K probably associates with bubbles system transformation caused by high mobility of vacancies.

REFERENCES

1. Yang Zhanbing, Hu Benfu, H. Kinoshita, H. Takahashi, S. Watanabe. Effect of hydrogen ion/electron dual-beam irradiation on microstructural damage of a 12Cr-ODS ferrite steel // *J. Nucl. Mater*. 2010, v. 398, p. 81-86.

2. G.D. Tolstolutskaya, V.V. Rushytskiy, I.E. Kopanets, S.A. Karpov, V.V. Bryk, V.N. Voyevodin, F.A. Garner. Displacement and helium-induced enhancement of hydrogen and deuterium retention in ion-irradiated 18Cr10NiTi stainless steel // *J. Nucl. Mater*. 2006, v. 356, p. 136.

3. G.D. Tolstolutskaya, V.V. Ruzhytskiy, S.A. Karpov, I.E. Kopanets. Features of retention and release of deuterium out of radiation-induced damages in steels // *Problems of atomic science and technology. Series "Physics of Radiation Effect and Radiation Materials Science"*. 2009, N 4-1(62), p. 29-41.

4. S.A. Karpov, V.V. Ruzhytskiy, I.M. Neklyudov, V.I. Bendikov, G.D. Tolstolutskaya. Parameters of trapping and thermally activated release of deuterium ion-implanted in 18Cr10NiTi steel // *Metalofizika I Noveishie Teknologii*. 2004, N 12, p. 1661-1670 (in Russian).

5. N. Marochov, P.J. Goodhew. A comparison of the growth of helium and neon bubbles in nickel // *J. Nucl. Mater.* 1988, v. 158, p. 81.

6. www.srim.org.

7. A.P. Druzhkov, V.L. Arbuzov, D.A. Perminov. Positron annihilation study of effects of Ti and plastic deformation on defect accumulation and annealing in electron-irradiated austenitic steels and alloys // *J. Nucl. Mater.* 2005, v. 341, p. 153-163.

8. J. Arunkumar, S. Abhaya, R. Rajaraman, et al. Defect recovery in proton irradiated Ti-modified stainless steel probed by positron annihilation // *J. Nucl. Mater*. 2009, v. 384, p. 245-248.

9. P. Wang, Y. Li, J. Liu, G. Zhang, R. Ma, P. Zhu, C. Qiu, T. Xu. A study of helium trapping, bubble structures and helium migration in type 316L stainless steel under helium implantation // *J. Nucl. Mater*. 1989, v. 169, p. 167.

10. A.A. Gadalla, W. Jäger, P. Ehrhart. TEM investigation of the microstructural evolution during mev helium implantation in copper // *J. Nucl. Mater*. 1985, v. 137, p. 73.

Статья поступила в редакцию 18.06.2014 г.

СОВМЕСТНОЕ ВЛИЯНИЕ РАДИАЦИОННЫХ ПОВРЕЖДЕНИЙ И ПРИМЕСЕЙ ИНЕРТНЫХ ГАЗОВ НА УДЕРЖАНИЕ ДЕЙТЕРИЯ В АУСТЕНИТНЫХ И ФЕРРИТНО-МАРТЕНСИТНЫХ СТАЛЯХ

С.А. Карпов, И.Е. Копанец, В.В. Ружицкий, Б.С. Сунгуров, Г.Д. Толстолуцкая

Изучено поведение водорода (дейтерия) в аустенитной нержавеющей стали Х18Н10Т и ферритно-мартенситных сталях ЕР-450 и ЕІ-852. Для моделирования дефектной структуры, которая образуется в материалах ядерных энергетических установок, использовали облучение сталей высокоэнергетичными ионами аргона. Влияние предварительного облучение аргоном на удержание дейтерия в сталях исследовали методами ионной имплантации, ядерных реакций $D(^3He,p)^4He$, термодесорбционной спектроскопии и просвечивающей электронной микроскопии. Было установлено, что удержание дейтерия в сталях существенно повышается в присутствии радиационных повреждений, созданных предварительной имплантацией ионов аргона. Наблюдается сдвиг температурного интервала выхода водорода из кристаллической решетки на 200 К в область более высоких температур. Для извлечения термодинамических параметров захвата и десорбции дейтерия из сталей использовалась расчетная модель, основанная на теории диффузии атомов водорода в поле радиационных дефектов.

СПІЛЬНИЙ ВПЛИВ РАДІАЦІЙНИХ ПОШКОДЖЕНЬ І ДОМІШОК ІНЕРТНИХ ГАЗІВ НА УТРИМАННЯ ДЕЙТЕРІЮ В АУСТЕНІТНИХ І ФЕРИТНО-МАРТЕНСИТНИХ СТАЛЯХ

С.О. Карпов, І.Є. Копанець, В.В. Ружицький, Б.С. Сунгуров, Г.Д. Толстолуцька

Вивчено поведінку водню (дейтерію) в аустенітній нержавіючій сталі Х18Н10Т і феритно-мартенситних сталях ЕР-450 і ЕІ-852. Для моделювання дефектної структури, що виникає в матеріалах ядерних енергетичних установок, використовували опромінення сталей високоенергетичними іонами аргону. Вплив попереднього опромінення аргоном на утримання дейтерію в сталях досліджували методами іонної імплантації, ядерних реакцій $D(^3He,p)^4He$, термодесорбційної спектроскопії та просвічуючої електронної мікроскопії. Було встановлено, що утримання дейтерію в сталях істотно зростає в присутності радіаційних пошкоджень, створених попередньою імплантацією іонів аргону. Спостерігається зміщення температурного інтервалу виходу водню з кристалічної решітки на 200 К в область більш високих температур. Для отримання термодинамічних параметрів захоплення і десорбції дейтерію із сталей використовувалася розрахункова модель, заснована на теорії дифузії атомів водню в полі радіаційних дефектів.